

# Theoretical and experimental analysis of the lateral modes of high-power broad-area lasers

H. Wenzel\*, P. Crump\*, H. Ekhteraei\*, C. Schultz\*, J. Pomplun†, S. Burger‡†, L. Zschiedrich†, F. Schmidt‡† and G. Erbert\*

\* Ferdinand-Braun-Institut, Leibniz-Institut für Höchstfrequenztechnik, Gustav-Kirchhoff-Str. 4, 12489 Berlin, Germany

† JCMwave GmbH, Bolivarallee 22, 14050 Berlin, Germany

‡ Zuse-Institut Berlin, Takustr. 7, 14195 Berlin, Germany

**Abstract**—For maximum fiber-coupled power, broad-area (BA) diode lasers must operate with small lateral far field angles. However, these structures are laterally multi-moded, with low beam quality and wide emission angles. We use a combination of device simulation and diagnostic measurements to determine the physical factors limiting the lateral far field angle in state of the art BA lasers emitting at 975 nm. Two-dimensional simulations of the optical field enable the dominant lateral waveguiding mechanisms to be diagnosed. Spectrally resolved near and far field measurements will allow us to determine the nature of the lateral modes.

## I. INTRODUCTION

High-power diode lasers offer several advantages compared to solid-state and gas lasers such as high conversion efficiency, small size and ease of handling. Due to the large lateral emission aperture of typically 100  $\mu\text{m}$  in order to ensure a reliable operation at 10 W output power and above [1], these devices operate in multiple lateral modes, limiting how effectively they can be laterally collimated and fiber coupled.

The lateral modes are induced by several physical effects, specifically: (a) built-in refractive index profiles from structures such as etched trenches or impurity induced disordering, (b) gain, loss and associated anti-index profiles arising from the injected carrier density, (c) self heating (thermal lensing) mainly induced by the current flowing through the device. Self-focusing effects can also form non-linear modes, typically called filaments. In all cases, higher currents lead to more lateral modes and wider far fields, degrading the beam quality, with typically behavior shown in Fig. (1) for one example device. The full far field angle (95% power inclusion) increases from 3.5° to 11° as the power is increased from 0.5 W to 10 W. Moreover, the multi-peaked, irregular profile indicates the presence of many lateral modes.

A rigorous diagnosis of the lateral waveguiding mechanism would assist in developing new designs with smaller far fields. Our intention here is to use a combination of device simulation and diagnostic measurements to determine the physical factors limiting the lateral far field angle in state of the art broad-area (BA) lasers emitting at 975 nm.

## II. THEORETICAL MODEL AND NUMERICAL RESULTS

To our knowledge, there are no tools available, which allow a comprehensive simulation of multi-moded diode lasers taking into account self-consistently waveguiding, drift-diffusion

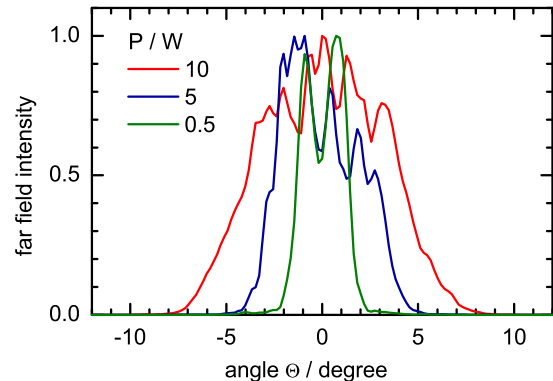


Fig. 1. Measured profiles of the lateral far field intensity at output powers of 0.5, 5 and 10 W. Stripe width and cavity length are  $W = 90 \mu\text{m}$  and  $L = 4 \text{ mm}$ , respectively. Facet reflectivities are 1% and 95%.

of carriers and heat flow in the transverse plane. Therefore, in the present stage of the diagnostics we use a restricted model which includes only waveguiding and heat flow. We will show by a comparison with experimental results that thermal lensing is the dominant lateral waveguiding mechanism at high optical output. As a consequence of the limitations of the model, we have to make some ad-hoc assumptions about the distribution of the heat sources and the carrier-density dependent part of the dielectric function.

For the computations we use the software JCMSuite which solves the stationary, complex-valued Maxwell's equations numerically with an adaptive finite element approach [2] to determine the modes in the transverse plane. In order to account for the temperature induced change of the refractive index, it has been supplemented by a model for the heat flow, which is treated again by an adaptive finite element approach, but on a larger domain and another grid than that for the Maxwell's equations. As a result of the numerical solution of the heat flow equation we obtain the temperature distribution  $T(x, y)$ , which is translated into a corresponding distribution of the index change by the relation

$$\Delta n = \frac{dn}{dT}(T - T_0), \quad (1)$$

where  $T_0$  is the reference temperature of the refractive indices which is typically equal to the heat sink temperature. The change of index with temperature  $dn/dT = 2.5 \times 10^{-4}$  [3] is assumed to be temperature independent and spatially constant.

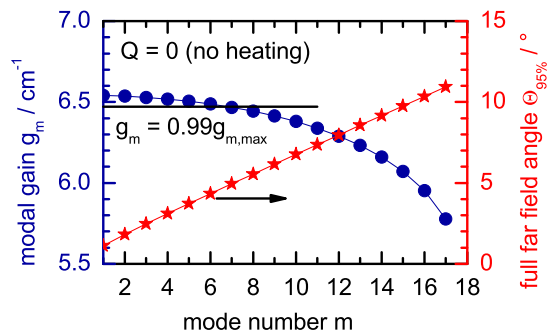


Fig. 2. Calculated modal gain (bullets, left axis) and lateral far field angle (95% power inclusion, right axis) versus mode number. No heating.

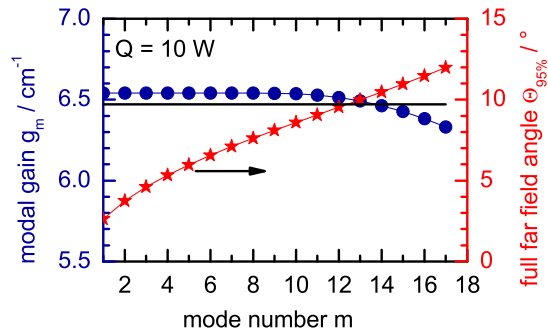


Fig. 3. Calculated modal gain (bullets, left axis) and lateral far field angle (95% power inclusion, right axis) versus mode number. 10 W thermal power.

Figs. 2 and 3 show results of an example computation. Stripe width and cavity length is the same as in fig. 1. For the case of vanishing self-heating the modal gain rapidly decreases with increasing mode number. The full far-field angle (95% power inclusion) rises linearly with the mode number. Using the (artificial) criterium that the modal gain of lasing modes should not deviate more than 1% from each other, there are 6 lasing modes. The 6th mode has a far field angle of 4.3°.

When self-heating is taken into account, the modal gain remains almost constant for a large number of modes and the far field angle increases in a super-linear manner with mode number. Using the same criterium as above, there are now 13 potential lasing modes. The 13th mode has a far field angle of 10°. However, the far field of each mode is wider, too. For example, the 6th mode has now a far field angle of 6.5°. Assuming an incoherent superposition of the fields of the individual modes, clearly the observed widening of the lateral far field can be attributed both to an increased number of lateral modes and to a widening of the lateral far field of each mode.

### III. OUTLOOK

Provided the lateral modes are incoherent, it is possible to experimentally separate them and determine both their spatial profile (near field) and their far field profiles. The profiles of the lateral optical modes can be determined using the fact that each mode has a different effective index, so that the comb of the longitudinal modes corresponding to one lateral mode is shifted spectrally with respect to the comb of another lateral mode. Typically, a high-resolution spectrometer can be used to

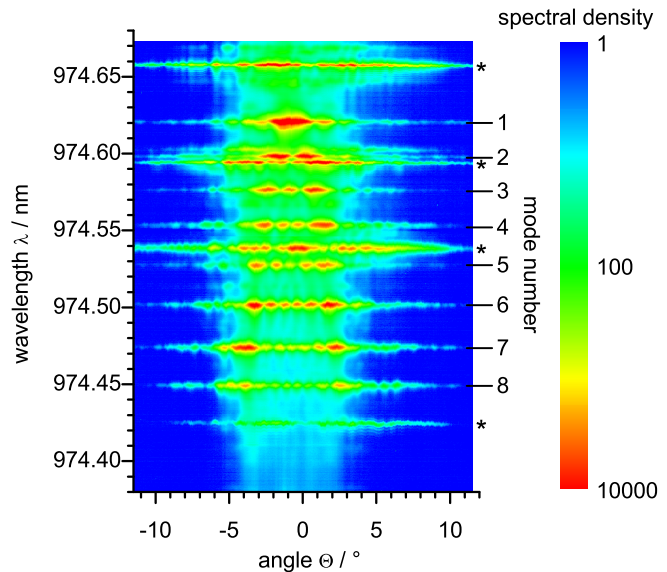


Fig. 4. Mapping of measured power spectral density drawn on a logarithmic scale versus lateral angle (horizontal axis) and wavelength (vertical axis). The ticks on the right hand side are labeled with the mode numbers identified. The output power is  $P = 2.5$  W and the cavity length is  $L = 3$  mm.

experimentally separate them. In practice, in broad-area lasers each spectral line splits into multiple peaks, corresponding to the different lateral modes belonging to one longitudinal mode, because their effective indices differ not so much. However, especially for large cavity lengths the wavelengths of the lateral modes corresponding to different longitudinal modes overlap and can not be experimentally separated, so that it is advantageous to investigate distributed feedback (DFB) BA lasers where ideally only a single longitudinal mode lases.

As an illustrative example Fig. 4 shows the result of a spectrally resolved measurement of the profile of the lateral far field intensity of an index-guided DFB BA laser [4]. We should note, that the entire spectrum and all observed modes are shown. Eight modes can be clearly identified by counting the number of the main intensity maxima, which are labeled correspondingly in Fig. 4. On average the lateral modes are separated by 24 pm, with slightly greater values for larger mode numbers. There are four additional lateral modes belonging to the adjacent longitudinal mode. At the conference, we will present further results and comparisons with simulations.

### REFERENCES

- [1] P. Crump, G. Blume, K. Paschke, R. Staske, A. Pietrzak, U. Zeimer, S. Einfeldt, A. Ginolas, F. Bugge, K. Häusler, P. Ressel, H. Wenzel, G. Erbert, "20W continuous wave reliable operation of 980nm broad-area single emitter diode lasers with an aperture of 96 $\mu$ m," *Proc. SPIE*, vol. 7198, p. 719814, 2009.
- [2] J. Pomplun, S. Burger, L. Zschiedrich, F. Schmidt, "Adaptive finite element method for simulation of optical nano structures," *pss (b)*, vol. 244, no. 10, pp. 3419-3434, Oct. 2007.
- [3] A.I. Bawamia, B. Eppich, K. Paschke, H. Wenzel, F. Schnieder, G. Erbert, G. Tränkle, "Experimental determination of the thermal lens parameters in a broad area semiconductor laser amplifier," *Appl. Phys. B*, vol. 97, no. 1, pp. 95-101, 2009.
- [4] C.M. Schultz, P. Crump, H. Wenzel, O. Brox, A. Maaßdorf, G. Erbert, G. Tränkle, "11W broad area 976 nm DFB lasers with 58% power conversion efficiency," *Electron. Lett.*, vol. 46, no. 8, pp. 580-581, 2010.